Schistosoma haematobium infection is associated with alterations in energy and purine-related metabolism in preschool-aged children

Derick N. M. Osakunor[1]*, **Takafira Mduluza**[2], **Douglas Osei-Hyiaman**[3,4,5†], **Karl Burgess**[6], **Mark E. J. Woolhouse**[7,8], **Francisca Mutapi**[1,8]

1 Institute of Immunology & Infection Research, University of Edinburgh, Ashworth Laboratories, King's Buildings, Edinburgh, United Kingdom, **2** Biochemistry Department, University of Zimbabwe, Mount Pleasant, Harare, Zimbabwe, **3** Laboratory of Physiologic Studies, National Institute on Alcohol Abuse and Alcoholism, National Institutes of Health, Bethesda, Maryland, United States of America, **4** Metabolomics Research Division, Human Metabolome Technologies Inc., Tsuruoka, Yamagata, Japan, **5** Department of Systems Neurophysiology, Graduate School of Medical & Dental Science, Tokyo Medical and Dental University, Bunkyo City, Tokyo, Japan, **6** Centre for Synthetic and Systems Biology, University of Edinburgh, CH Waddington Building, King's Buildings, Edinburgh, United Kingdom, **7** Usher Institute, University of Edinburgh, Ashworth Laboratories, King's Buildings, Edinburgh, United Kingdom, **8** NIHR Global Health Research Unit Tackling Infections to Benefit Africa (TIBA), University of Edinburgh, Ashworth Laboratories, King's Buildings, Edinburgh, United Kingdom

† Deceased.
* d.osakunor@ed.ac.uk

Abstract

Helminths are parasitic worms that infect over a billion people worldwide. The pathological consequences from infection are due in part, to parasite-induced changes in host metabolic pathways. Here, we analyse the changes in host metabolic profiles, in response to the first Schistosoma haematobium infection and treatment in Zimbabwean children. A cohort of 83 schistosome-negative children (2–5 years old) as determined by parasitological examination, guardian interviews and examination of medical records, was recruited at baseline. Children were followed up after three months for parasitological diagnosis of their first S. haematobium infection, by detection of parasite eggs excreted in urine. Children positive for infection were treated with the antihelminthic drug praziquantel, and treatment efficacy checked three months after treatment. Blood samples were taken at each time point, and capillary electrophoresis mass spectrometry in conjunction with multivariate analysis were used to compare the change in serum metabolite profiles in schistosome-infected versus uninfected children. Following baseline at the three-month follow up, 11 children had become infected with S. haematobium (incidence = 13.3%). Our results showed that infection with S. haematobium was associated with significant increases (>2-fold) in discriminatory metabolites, linked primarily with energy (G6P, 3-PG, AMP, ADP) and purine (AMP, ADP) metabolism. These observed changes were commensurate with schistosome infection intensity, and levels of the affected metabolites were reduced following treatment, albeit not significantly. This study demonstrates that early infection with S. haematobium is associated with alterations in host energy and purine metabolism. Taken together, these changes

are consistent with parasite-related clinical manifestations of malnutrition, poor growth and poor physical and cognitive performance observed in schistosome-infected children.

Author summary

Schistosomiasis is a parasitic disease caused by helminth worms called schistosomes, and millions of people worldwide are infected. Studies in animal models indicate that the infection can cause alterations in metabolism of the host, leading to the observed clinical manifestations of the disease. However, there are limited human studies on the impact of schistosome infection on host metabolism, and none describing the changes that occur early in infection. There are also no studies relating to the species *Schistosoma haematobium*, which causes disease manifested in both the urinary and genital organs. To address this, we analysed the metabolic changes in response to the first *S. haematobium* infection and treatment in Zimbabwean preschool-aged children. We determined for the first time, that within three months of first infection, there are significant changes in metabolite profiles related to host energy (G6P, 3-PG, AMP, ADP) and purine (AMP, ADP) metabolism. These changes were associated with infection burden and were resolved within three months, following curative treatment. Our findings provide further understanding into the early host metabolic responses to the infection, consistent with clinical manifestations such as malnutrition, poor growth and poor physical and cognitive performance observed in schistosome-infected children. This demonstrates the need for early treatment of the infection, and will inform the development of appropriate interventions such as nutraceuticals in child feeding programs, aimed at reducing disease consequences. Further mechanistic studies will contribute to more understanding of the relationship between metabolic alterations and schistosomiasis in young children.

Introduction

Helminths are multicellular parasitic worms that infect over a billion people worldwide [1]. In tropical and sub-tropical regions with limited access to safe water and adequate sanitation provision, diseases caused by helminth infections including soil-transmitted helminths (STH) [1] and schistosomes are highly prevalent [2–4]. With an estimated 250 million people infected worldwide, schistosomiasis is a parasitic disease caused by helminth trematodes of the *Schistosoma* genus [5]; at least 90% of all cases occur in sub-Saharan Africa [6,7]. The species *Schistosoma haematobium*, accounts for about two-thirds of all schistosomiasis cases in Africa, and causes the urogenital form of the disease [8,9]. Diagnosis is typically by microscopic detection of eggs in urine, and treatment is by administration of the anti-helminthic drug, praziquantel [9].

In endemic areas with high infection transmission, infection with schistosomes is cumulative, and can begin in the first year of birth [10]. The health impacts of *S. haematobium* infection thus begin at this early age and can include haematuria, protein wasting [11–13], malnutrition, poor growth, and poor physical and cognitive performance [14]. Left untreated, infection can lead to chronic disease and pathology, including anaemia, poor reproductive health, increased susceptibility to sexually transmitted infections [14], prostate cancer [15], urothelial carcinogenesis [16], bladder dysfunction, fibrosis, and renal failure [17].

Interaction between the schistosome worm and its host is central to parasite survival. Successful parasitic relationships can thus be achieved by manipulating the host's metabolism to

divert essential nutrients and metabolites towards parasite growth. For instance, schistosome worms rely on host glucose as their main source of energy for survival [18,19]. In addition, schistosome infection induces parasite-specific immune responses that cause a downregulation and immuno-modulation of the host's immune system, to promote parasite survival for decades [20–23]; the alteration in host immune responses can alter host metabolic function, disease patterns and overall host health [24]. Experimental schistosome studies have shown that in order to establish themselves and survive in the host (including growth, development and egg laying), schistosome worms require host-derived endocrine steroid and thyroid hormones [25–27], as well as immune molecules including tumour necrosis factor alpha [28,29], interleukin-7 [25], and CD4+ T lymphocytes [30]. When such host factors are unavailable to the parasite, there is poor parasite development and fecundity, and infection causes reduced pathology in the host [31–33]. Taken together, the available experimental evidence indicates that the alterations in systemic host pathways extend to metabolism. Current evidence from mouse models of schistosomiasis show that schistosome infection and disease are linked to alterations in gut microbiota metabolism [19,34], as well as changes in amino acid, lipid and energy metabolism [19,34–36]. Alterations in liver metabolism due to parasite egg-induced inflammatory responses have also been reported [37]. Studies characterising the metabolic changes to human schistosome infection are limited. However, analysis of urine samples has been recently applied to study the host metabolic changes in *S. mansoni*-infected children and adults [38,39]. The findings were similar to those from experimental models in terms of alterations in energy, liver, and gut microbiota metabolism, all of which are linked to morbidity from the infection [38,39].

While the significant detrimental effects of schistosome infections on host health are unarguable, some experimental and human epidemiological studies have suggested that the sustained host metabolic alterations from schistosome infections may reduce the occurrence and severity of other conditions, including metabolic syndrome [19,40–43]. The exact mechanisms of these effects remain to be fully understood [23]. It is clear that there is a need for further studies on the dynamics of host-parasite relations at the molecular level, to elucidate pathways involved in pathology and disease progression versus those ameliorating metabolic syndromes.

In the case of *S. haematobium* infection in infants and young children, little is known about the basic mechanisms underlying the pathophysiology of the disease [44]. There are limited human studies on the impact of schistosome infection on host metabolism, and metabolic phenotyping of blood samples from cases of human schistosomiasis has not been reported. The majority of previous investigations both in human and animal models have been based on well-established late stage schistosome infections; this does not allow the early metabolic changes associated with the first schistosome infection to be elucidated. The currently available evidence have also focused on *S. mansoni* and *S. japonicum* infections, and there have not yet been any published studies on the impact of human *S. haematobium* infection, on the host metabolic phenotype. Thus, this study aims to characterise the host metabolite profiles of Zimbabwean preschool-aged children (≤5 years) before their first *S. haematobium* infection, and the changes that occur following infection and treatment. It further determines the impact of such specific metabolite alterations on host metabolism and the development of schistosome-related morbidity. We hypothesised that early in the first *S. haematobium* infection in preschool-aged children, there are alterations in host metabolite profiles linked with metabolic pathways implicated in schistosome-related morbidity.

Methods

Ethics statement

Ethical and institutional approval for the main study (of which this is a subset) was obtained from the Medical Research Council of Zimbabwe (MRCZ/A/1964) and the University of

Edinburgh (fmutapi-0002), respectively. The Medical Director of the Mashonaland Central Province also granted permission to conduct the study in the area. The study aims and procedures were explained to participants' parents/guardians in Shona, the local language, and participation in the study was voluntary. Written informed consent was obtained from the participants' parents/guardians.

Study design, population and site

The study followed a longitudinal design, embedded within a larger paediatric urogenital schistosomiasis study conducted in the Shamva district, Northeast Zimbabwe. The study was designed to detect the first schistosome infection in preschool-aged children, and to determine the health impact of infection and treatment as previously published [13]. The study area, Madziwa (17˚04′S 31˚40′E), was chosen because a previous national survey showed that the area has a high prevalence of *S. haematobium* (>50%), and a low prevalence of *S. mansoni* and STH (<15%) [45].

While in experimental studies it is possible to infect animals at specific time points, follow the course of infection, and investigate its impact on the host, this is not possible in human hosts. Hence in the current study, we followed natural infection of populations living in schistosome-endemic areas. The study included 83 children, aged 2–5 years, not previously infected or treated for schistosomiasis (assessed by health questionnaire and clinical records) and confirmed schistosome negative (by egg count for *S. haematobium* and *S. mansoni*). The children were also diagnosed for other helminths to exclude STH infections via stool examination (by egg count). At baseline, a questionnaire was administered at recruitment to gather metadata on basic socio-demography and anthropometric measurements including height, weight, and mid-upper arm circumference (MUAC) as previously described [13]. A venous blood sample was also collected from each child and later processed to collect serum for metabolite analysis. Children were then followed up three months later to detect their first *S. haematobium* infection (by egg count). At this follow up survey, a second blood sample was collected from all children for analysis to detect changes in metabolite profiles from baseline. Both experimental and previous field studies show that in three months, any new *S. haematobium* infections acquired would have reached patency and thus be detectable by egg excretion in urine [46–48]. All children who were positive for *S. haematobium* infection were treated by clinical staff (local nurses from the Madziwa rural clinic) with a single dose of praziquantel at the standard 40 mg/kg body weight as previously described [4]. For treated children, a post-treatment efficacy check (by egg count) and blood sampling was carried out three months later. Fig 1 shows a summary of the study design.

Sample collection and processing

Parasitology samples. For schistosomiasis diagnosis, approximately 50 mL of urine was collected on three consecutive days at each time point, and a stool specimen was collected on a single day at baseline. Urine samples were examined microscopically for *S. haematobium* infection following the standard urine filtration procedure [49], and infection intensity was reported as the arithmetic mean number of eggs per 10 mL urine of at least two urine samples. The stool samples collected were processed using the Kato–Katz method (in duplicates) [50], and parasite eggs enumerated microscopically to exclude *S. mansoni* and STH. Children were positive for infection if at least one parasite egg was detected in at least one of the urine or stool samples.

Blood samples. Up to 5 mL of venous blood was collected from each participant, allowed to clot at room temperature for about 30 minutes, and stored at 4˚C for a maximum of 4 hours.
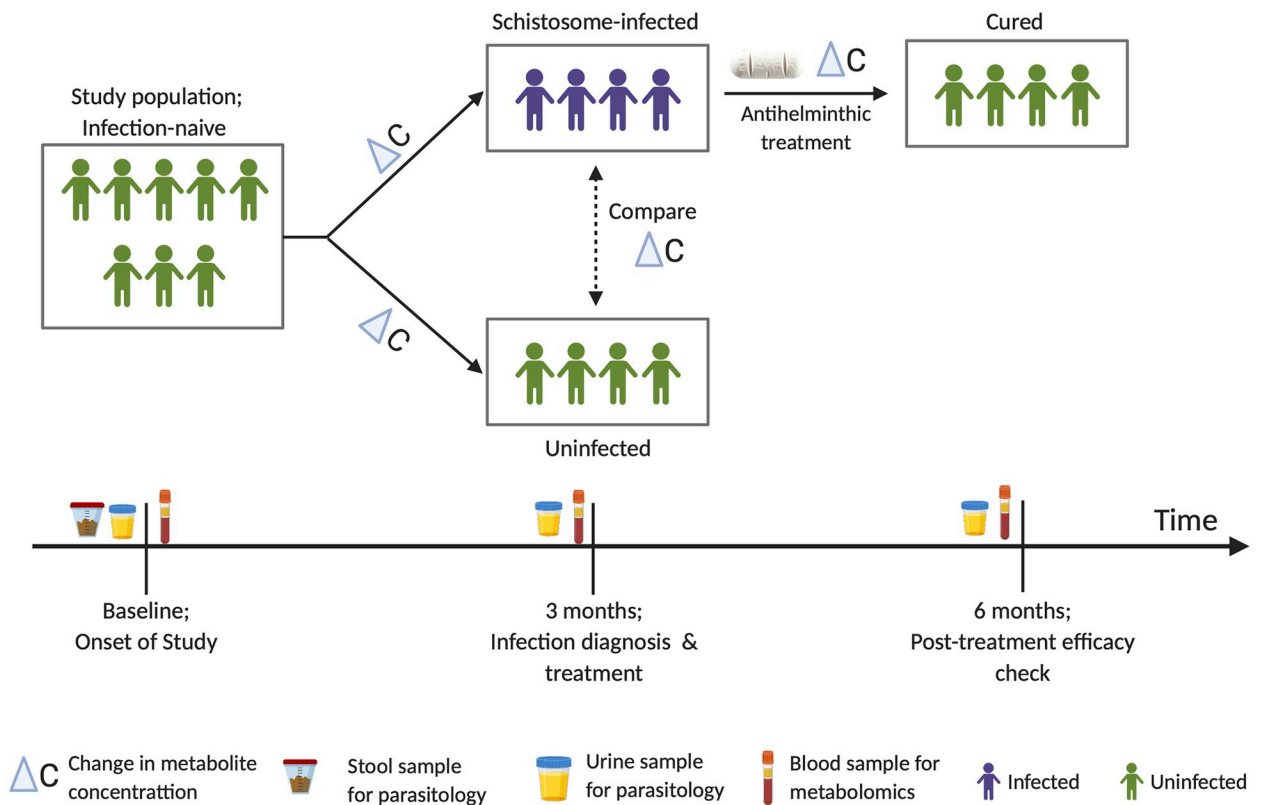
Fig 1. Summary of study design. Schistosome-infected and uninfected refer to diagnosis by microscopic egg counts in urine.

https://doi.org/10.1371/journal.pntd.0008866.g001

Serum was obtained from the samples after centrifugation at 3000 rpm for 10 minutes, frozen at -20˚C in the field and transferred to a −80˚C freezer in the laboratory (University of Zimbabwe), prior to cold-chain shipment to the University of Edinburgh, UK. For long-term storage, samples were kept at −80˚C until shipped on dry ice to Human Metabolome Technologies Inc. (HMT; Yamagata, Japan) for metabolite analysis. Appropriate pre-analytical considerations for processing blood samples for metabolite analysis were followed [51]. Blood samples were collected rather than urine samples for metabolite analysis because blood is less susceptible to metabolite variations related to sample collection time, meal intake and hydration levels [52]. To minimise the effects of meal and sample-time factors on metabolite analysis, non-fasting pre-meal samples were collected at about midday during recruitment [52].

Metabolite measurements: CE–TOF–MS.   Sample preparation and metabolite analysis was carried out by HMT using the capillary electrophoresis time-of-flight mass spectrometry (CE–TOF–MS)-based metabolomics technique [53,54]. 50 μL of serum sample was mixed with 450 μL of methanol containing 10 μM internal standards. Chloroform (500 μL) and Milli-Q water (200 μL) were added, mixed thoroughly and centrifuged (2,300 x g, 4˚C for 5 minutes). The water layer (400 μL) was filtered through a 5-kDa cut-off filter (ULTRA-FREE-MC-PLHCC; HMT, Yamagata, Japan) to remove macromolecules. The filtrate was concentrated by centrifugation and resuspended in 50 μL of ultrapure water immediately before measurement. Spectra profiles were obtained using a CE–TOF–MS (Agilent Technologies Inc. Waldbronn, Germany) system. Full details of experimental conditions and instrumentation are as previously described [55–57] (details described in S1 Text).

CE-TOF-MS data acquisition and processing. Peak information including mass-to-charge ratio (*m/z*), migration time (MT), and peak area, were extracted using automatic integration software (MasterHands ver. 2.17.1.11 developed at Keio University). Relative peak area was calculated using a peak detection limit based on signal-noise ratio (S/N) = 3 [57]:

$$Relative\ Peak\ Area\ =\ \frac{Metabolite\ Peak\ Area}{Internal\ Standard\ Peak\ Area \times Sample\ Amount} \tag{1}$$

For peak annotation, putative metabolites were then assigned from HMT's standard library and Known-Unknown peak library based on *m/z* and MT. In instances where a feature matched with multiple annotations within their m/z and MT windows, all alternatives are provided. The tolerance level was ±0.5 min in MT and ±10 ppm in *m/z* [56].

$$Mass\ error\ (ppm)\ =\ \frac{Measured\ Value - Theoretical\ Value}{Measured\ Value} \times 10^6 \tag{2}$$

Using standard curves obtained by single-point (100 μM) calibrations, absolute metabolite concentrations were calculated by normalizing the peak area of each metabolite with respect to the area of the internal standard. This minimised technical variability and also enabled sample to sample comparisons in data analysis.

A total of 248 metabolite peaks (145 in cation and 103 in anion mode respectively) were detected and annotated based on HMT's standard and Known-Unknown peak library. Of these, 70 target metabolites were detected and quantified (40 in cation and 30 in anion mode respectively), and these were used for all downstream analysis. Individual samples for which a target peak or metabolite was below detection limits and thus could not be quantified, the peak area or concentration of the metabolite was captured as "Not detected (N.D)".

Data analyses

Data analyses and visualisations were performed using SPSS version 22 (IBM Corp.), GraphPad Prism version 8.2.0 (GraphPad Software, Inc), and MetaboAnalyst, a web-based tool for the analysis of metabolomic data [58–60]. Continuous data are presented as mean (standard deviation; SD) or as median (interquartile range; IQR). Categorical data are presented as absolute numbers and percentages.

Prior to analysis, a data integrity check was performed (MetaboAnalyst), and missing values (in this case "N.D") caused by metabolites below the detection limit were replaced by a small value (i.e. half the minimum positive value in the data set = 0.15 μM), as per standard practice in MetaboAnalyst (details in S1 Text). For changes in metabolite concentrations in response to schistosome infection, the change in metabolite concentrations (ΔC) at baseline (C1) and at follow up (C2) for infection was calculated as ΔC μM = C2 –C1 (μM). By default, MetaboAnalyst removes data for metabolites with a constant or a single value across samples. For metabolite analysis at baseline, six metabolites were found and removed. Likewise, to improve statistical power for metabolite analysis of the change in metabolite profile data, eight additional metabolites with less than n = 10 non-zero change in concentration values (ΔC) across samples were excluded from analysis with the change in concentration data set (14 metabolites in total) [details in S1 Text]. For all analyses, data were processed by range scaling [61].

To determine if the mean differences in metabolite profiles between groups of interest were likely due to chance, Multivariate Analysis of Variance (MANOVA; SPSS) with sequential sums of squares was used, as recommended for pathogen-related studies [62]. The model to determine and account for underlying age and sex-related effects at baseline included age

(years), sex, and their interaction, in that order. To determine the change in metabolite concentration due to schistosome infection, a model including age (years), sex, infection status and their interactions, in that order was used. Where the variable of interest was found to be significant, the model was then re-run without the significant variable, and the residuals from the resulting model were saved and subjected to further analysis to identify discriminatory metabolites compared across that variable (MetaboAnalyst). This was to ensure that the confounding effects of other factors such as age and sex were already accounted for, prior to downstream analysis to determine the most relevant metabolites accounting for differences in metabolite profiles between groups of interest.

Residuals from metabolite concentration data (from MANOVA models) along with participant metadata were imported into MetaboAnalyst. Univariate analysis using fold change (FC) and pattern correlation analysis (Pearson's) were used to identify metabolites that are potentially significant in discriminating between two groups, and to show metabolite patterns of change under different conditions. A false discovery rate (FDR) threshold of <0.05 [63] and a concentration ratio (i.e. between two groups) of at least 2-fold was considered significant [64]. For an informative first-hand look at the data set, an unsupervised Principal Component Analysis (PCA) was employed to assess clustering trends and group separation in the data set. To identify specific metabolites accounting for differences in metabolite profiles between groups of interest, a supervised multiple regression analysis method, Orthogonal Projections to Latent Structures Discriminant Analysis (OPLSDA) [65] with Orthogonal Signal Correction (OSC) filtering [66], was used to discriminate groups and identify the differentially expressed metabolites that drive group separation. This supervised method has been shown to be more reliable at overcoming the limitations of heterogeneity associated with analysis of human metabolomic data, where PCA does not reveal changes in metabolite profiles across groups [39,67]. Cumulative model statistics, R^2Y (cum) and Q^2 (cum), were calculated for each model and used to assess the degree of fit and predictive reliability respectively [68]. The significance of the model was evaluated using permutation testing (n = 1000), with a p-value threshold of 0.05 [69]. For all valid OPLSDA models, a combination of a generated S-plot [absolute p(corr) >0.5] and the variable importance in the projection (VIP) values (VIP $\geq$1.5) were used to identify and select significant differentially expressed metabolites between groups [70]. To further determine the relationship between significant differentially expressed metabolites (identified from the *S. haematobium* infection status OPLSDA model) and infection intensity, range-scaled residuals from the change in concentration metabolite data set (from MANOVA) were regressed on the log-transformed infection intensity ($\log_{10}$ [egg count+1]).

To identify metabolic pathways associated with schistosome infection and facilitate further biological interpretation, metabolite pathway analysis was performed in MetaboAnalyst; this combines results from powerful pathway enrichment analysis with pathway topology analysis. Data for the significant differentially expressed metabolites identified from the infection status OPLSDA model were queried against associated *Homo sapien*s metabolic pathway libraries (downloaded on 04.06.2019), curated from Kyoto Encyclopedia of Genes and Genomes (KEGG; http://www.genome.jp/kegg/). Full details of analysis are in S1 Text.

Results

Population characteristics

As shown in Table 1, median age was 3 years (range; 2–5 years) and 41 (49.4%) of the children were female. At follow up, 11 (13.3%) were positive for *S. haematobium* infection with mean infection intensity of 0.8 (SEM = 0.3; 95% CI = 0.2–1.5) eggs/10 mL of urine.

Table 1. Participant characteristics.

Variable	Total	Female	Male
	Baseline		
Age (years)			
Median	3 (3–4)	3 (3–4)	3.5 (3–4.3)
2	8 (9.6)	4 (9.8)	4 (9.5)
3	35 (42.2)	18 (43.9)	17 (40.5)
4	25 (30.1)	14 (34.1)	11 (26.2)
5	15 (18.1)	5 (12.2)	10 (23.8)
Height (cm)	96.0 (91.0–102.0)	96.0 (91.5–98.0)	100.0 (91.0–104.0)
Weight (kg)	14.0 (12.7–16.0)	14.0 (12.1–15.0)	15.0 (13.0–16.0)
MUAC (cm)	15.0 (14.0–16.0)	14.6 (14.0–15.4)	15.0 (14.0–16.0)
Mean WHZ	-0.29 (1.29)	-0.30 (1.23)	-0.28 (1.36)
Mean WAZ	-0.59 (1.19)	-0.62 (1.23)	-0.56 (1.16)
Mean HAZ	-0.70 (1.38)	-0.69 (1.45)	-0.71 (1.33)
	Follow up (3 months)		
S. h Infection status			
Negative	72 (86.7)	34 (82.9)	38 (90.5)
Positive	11 (13.3)	7 (17.1)	4 (9.5)
S. h Infection intensity (eggs/10 mL urine)	0.8 (0.2–1.5)	0.5 (0.1–1.0)	1.1 (0–2.3)

Table shows the characteristics of the sample population at baseline and at follow up. Growth and nutritional indices adjusted for age and expressed as Z-scores [71] was calculated using the WHO Anthro software (version 3.0.1; http://www.who.int/childgrowth/en/). Data are expressed as median (IQR) or n (%), except for WHZ, WAZ, and HAZ, which are mean (SD). *S. haematobium* infection intensity is shown as mean (95% confidence interval). S. h., *S. haematobium*; WHZ, weight–for-height Z-scores; WAZ, weight–for-age Z-scores HAZ, height-for-age Z scores.

https://doi.org/10.1371/journal.pntd.0008866.t001

Baseline metabolic differences associated with age and sex

Initial MANOVA models were built using baseline metabolite profiles to identify any underlying variations in the study population, pre-infection, and also to identify any potential confounders. From the baseline model, metabolites were found to vary across sex, but not age. The model was then re-run with age only, and the residuals were used to identify specific metabolites that vary with sex (S1 Table). As shown in Fig 2, univariate FC analysis showed that the concentrations of 16 metabolites were lower/down-regulated ($\geq$2-fold) in females (Fig 2A), and pattern correlation analysis showed that metabolite concentrations tend to be higher in males (Fig 2B). Of the 16, seven metabolites showing this pattern were statistically significant; creatinine (p <0.001), citrulline (p <0.001), cis-asconitic acid (p = 0.004), gamma-aminobutyric acid (GABA; p = 0.006), sarcosine (p = 0.014), 2-oxoisovaleric acid (p = 0.040), and isocitric acid (p = 0.040). Creatinine (FDR <0.001) and citrulline (FDR <0.001) remained significant after an FDR correction. Output details from the FC and pattern correlation analysis are given in S2 and S3 Tables respectively.

Based on the univariate analysis, multivariate analysis was used to determine significant metabolites associated with sex. Initial PCA analysis with a model of five components explaining 64.2% of the variability was aimed at identifying clustering according to sex. The PCA model however did not show any clear clustering by sex (see S1 Fig). This reflects the heterogeneity of data associated with human studies [67], in contrast to animal models where in-bred animals may contribute to clustering within the first few components [34]. To unmask changes, a supervised OPLSDA model was used to identify significant
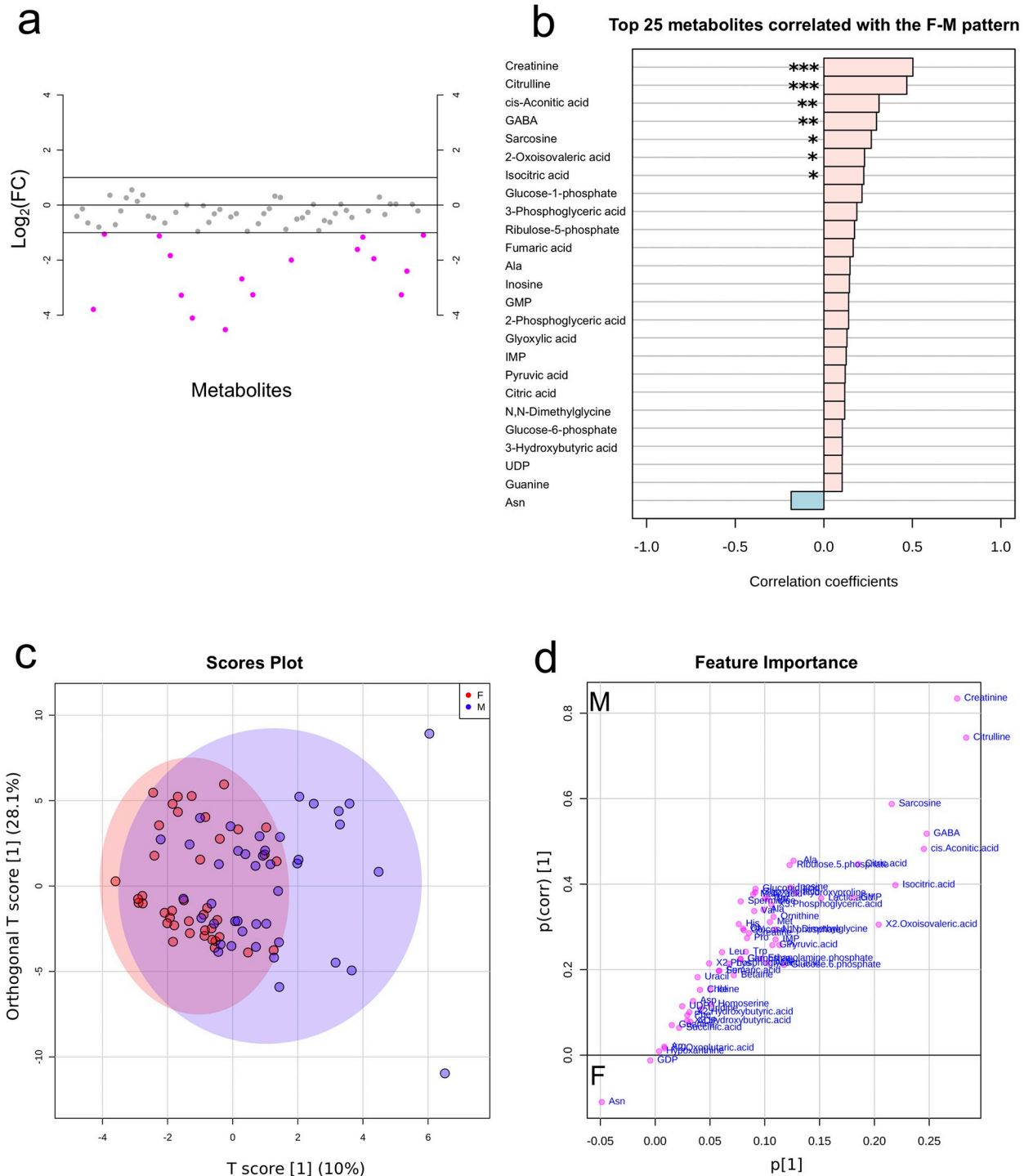
Fig 2. Metabolite profiles by sex. a) Metabolites identified by fold change (FC) analysis of female/male ratio with threshold of 2-FC. Values are on a log scale to show both up-regulated and down-regulated metabolites symmetrically. The plot shows metabolites that are up-regulated (positive-log scale) or down-regulated (negative log-scale). Pink symbols represent metabolites above the 2-FC threshold. b) Pattern correlation analysis showing metabolites (based on p-values) with different patterns between female and male (unadjusted top 7 metabolites significant; ***, p <0.001; **, p <0.01; *, p <0.05). Creatinine (FDR <0.001) and citrulline (FDR <0.001) remained significant after FDR correction. c) Score plot and d) Coefficient S-plot based on OPLSDA model of metabolite distribution according to sex (Y variable). Metabolites that significantly influenced the model (absolute p(corr) >0.5 and VIP ≥1.5) were creatinine, citrulline, sarcosine and GABA. For the S-plot, the y-axis represents the correlation or reliability coefficient and the x–axis represents the covariance or contributions of each metabolite to the model with respect to sex. GABA, gamma-aminobutyric acid; Ala, alanine; GMP, guanosine monophosphate; IMP, inosine monophosphate; UDP, uridine diphosphate; Asn, asparagine; F, female (n = 41); M, male (n = 42).

metabolites associated with sex (N = 83, 1 predictive and 1 orthogonal component; Q^2 = 0.146, p = 0.001 and R^2Y = 0.352, p = 0.033; see S2 Fig), from which a coefficient S-plot was used to identify significantly contributing metabolites discriminating between male and female. Based on the set selection criteria, males were observed to have increased concentrations of creatinine (p(corr) = 0.8, VIP = 2.9), citrulline (p(corr) = 0.7, VIP = 3.1), sarcosine (p(corr) = 0.6, VIP = 1.7), and GABA (p(corr) = 0.5, VIP = 2.4) compared to females [Fig 2C and 2D; see details in S4 Table].

Metabolic profiles during early schistosome infection

Due to the baseline variations in metabolite profiles related to sex, subsequent models to determine the change in metabolite profiles with schistosome infection were verified to account for potential bias. MANOVA models were built on change in metabolite profiles (ΔC) to determine any associations with *S. haematobium* infection, while accounting for age and sex. We found that *S. haematobium* status was associated with change in metabolite profiles (ΔC). For further downstream analysis, the model was re-run with age and sex only, and the residuals were used to identify metabolite features that vary by *S. haematobium* infection status (S5 Table). FC analysis showed that 25 metabolites were either up-regulated or down-regulated in schistosome infection more than 2-fold (Fig 3A), and metabolites showed either an increasing or decreasing pattern with schistosome infection status (Fig 3B). Of the 25, 16 metabolites showing this pattern were statistically significant. Metabolites that showed a pattern of increasing concentration with schistosome infection included adenosine diphosphate (ADP; p <0.001), 3-phosphoglyceric acid (3-PG; p <0.001), adenosine monophosphate (AMP; p <0.001), inosine (p = 0.012), asparagine (p = 0.016), 2-hydroxybutyric acid (p = 0.021), sarcosine (p = 0.023), guanosine monophosphate (GMP; p = 0.032); glucose-6-phosphate (G6P; p = 0.043), and ethanolamine phosphate (p = 0.043). Metabolites that showed a pattern of decreasing concentration with schistosome infection included lactic acid (p = 0.017), choline (p = 0.017), serine (p = 0.020), cis-asconitic acid (p = 0.023), histidine (p = 0.031), and glutamic acid (p = 0.045). ADP (FDR = 0.003), 3-PG (FDR = 0.003), and AMP (FDR = 0.014) remained significant after FDR correction. Output details from the FC and pattern correlation analysis are given in S6 and S7 Tables respectively.

Multivariate analysis was used to determine significant metabolites associated with schistosome infection. Initial PCA analysis with a model of five components explaining 57.5% of the variability, was used to identify clustering according to infection status. Likewise, the PCA model did not show any clear clustering by infection status (see S3 Fig), and heterogeneity in the data set may conceal metabolic changes characteristic of infection within the first few components [67]. To unmask such changes, a supervised OPLSDA model was used (N = 83, 1 predictive and 1 orthogonal component; Q^2 = 0.197, p = 0.001 and R^2Y = 0.465, p = 0.001; S4 Fig), from which a coefficient S-plot was used to identify significant metabolites discriminating between infected and uninfected children. Based on the selection criteria, *S. haematobium*-infected children were found to have increased concentrations of AMP (p(corr) = 0.7, VIP = 1.6), 3-PG (p(corr) = 0.7, VIP = 1.5), ADP (p(corr) = 0.6, VIP = 2.3), and G6P (p(corr) = 0.6, VIP = 1.5) [Fig 3C and 3D; see details in S8 Table].

Of interest, a MANOVA model to determine the influence of infection intensity on the significant metabolites identified by OPLSDA (accounted for age and sex) was significant (F-value = 5.178, p = 0.001; S9 Table). As shown in Fig 3E–3H, concentrations of all observed metabolites associated with schistosome infection status, increased as infection intensity increased. This relationship was significant for all metabolites except for G6P.
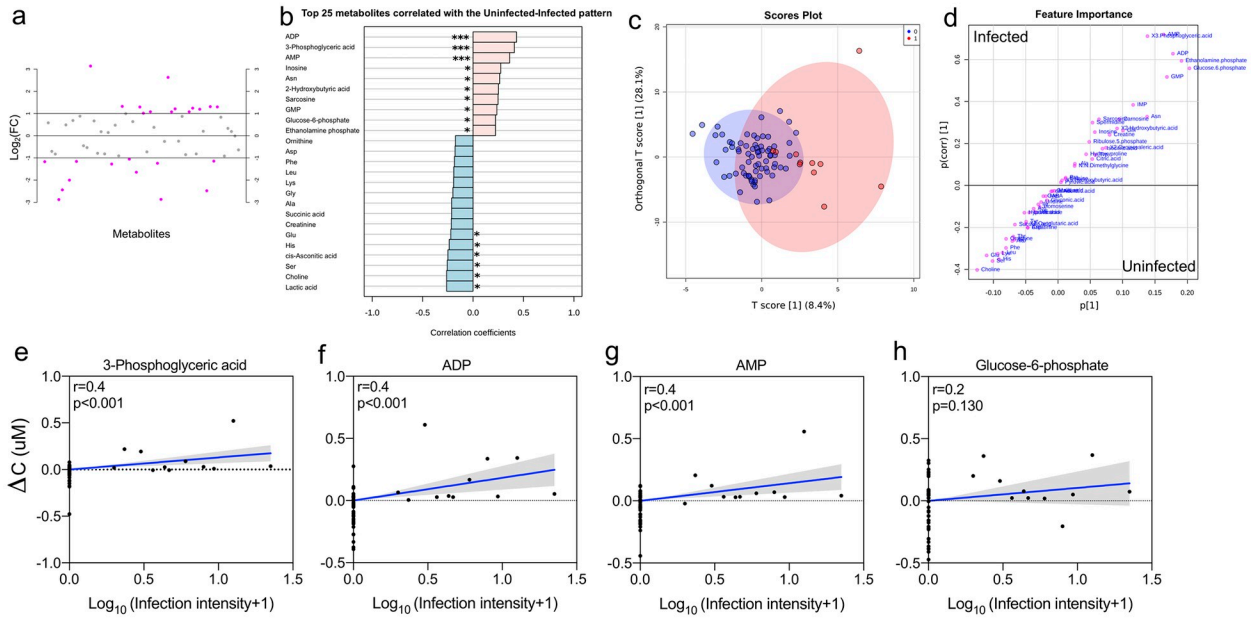
Fig 3. Metabolite profiles by schistosome infection status and intensity. a) Metabolites identified by fold change (FC) analysis by uninfected/ infected ratio with threshold of 2-FC. Values are on a log scale to show both up-regulated and down-regulated metabolites symmetrically. The plot shows metabolites that are up-regulated (positive-log scale) or down-regulated (negative log-scale). Pink symbols represent metabolites above the 2-FC threshold. b) Pattern correlation analysis showing the top 25 metabolites (based on p-values), showing increasing and decreasing patterns with schistosome infection status (unadjusted top 16 significant; ***, $p < 0.001$; **, $p < 0.01$; *, $p < 0.05$). ADP (FDR = 0.003), 3-phosphoglyceric acid (FDR = 0.003), and AMP (FDR = 0.014) remained significant after FDR correction. c) Score plot and d) coefficient S-plot based on OPLSDA model of metabolite distribution according to infection status (Y variable). Metabolites that significantly influenced the model (absolute p(corr) >0.5 and VIP ≥ 1.5) were AMP, 3-PG, ADP, and G6P. For the S-plot, the y-axis represents the correlation or reliability coefficient and the x–axis represents the covariance or contributions of each metabolite to the model with respect to infection status. e–h) Scatter plots showing linear regression analysis of infection intensity and change in metabolite concentration (ΔC) of the specific metabolites identified through OPLSDA as associated with schistosome infection status. Infection status was coded as 0 and 1 for uninfected (n = 72) and infected (n = 11) respectively, for n = 83 independent samples. *S. haematobium* infection intensity was log-transformed [$\log_{10}$ (egg count+1)]. Shaded areas indicate the 95% confidence intervals. ADP, adenosine diphosphate; AMP, adenosine monophosphate; Asn, asparagine; GMP, guanosine monophosphate; Asp, aspartic acid, Phe, phenylalanine; Leu, leucine; Lys, lysine; Gly, glycine; Ala, alanine; Glu, glutamic acid; His, histidine; Ser, serine, 3-PG, 3-phosphoglyceric acid; G6P, glucose-6-phosphate.

https://doi.org/10.1371/journal.pntd.0008866.g003

Metabolite changes return to pre-infection levels following treatment

Of the 11 *S. haematobium*-positive children, a post-treatment follow-up sampling was conducted three months later to determine treatment efficacy, with a follow up rate of 6/11 (54.5%). Cure rate and egg reduction rates (by egg counts) were 100% in the six children followed up, and the impact of treatment on the concentration of the observed metabolites was determined in these six children. As shown in the heat map in Fig 4A, pattern analysis across all three time points showed that metabolite concentrations increased at infection and reduced to pre-infection levels, post-treatment. Although not significant (p >0.05), pattern correlation analysis (Fig 4B) showed that metabolite features exhibit a decreasing trend from infection to when children are schistosome negative (by egg count) following treatment [see details in S10 Table].

Pathway effects of metabolite alterations associated with schistosome infection

The metabolite pathway analysis assigned metabolite compounds in a total of seven pathways, which were identified together as important for the host response to schistosome infection. As shown in Fig 5A, the predominant hits were energy and purine pathways involved in glycolysis
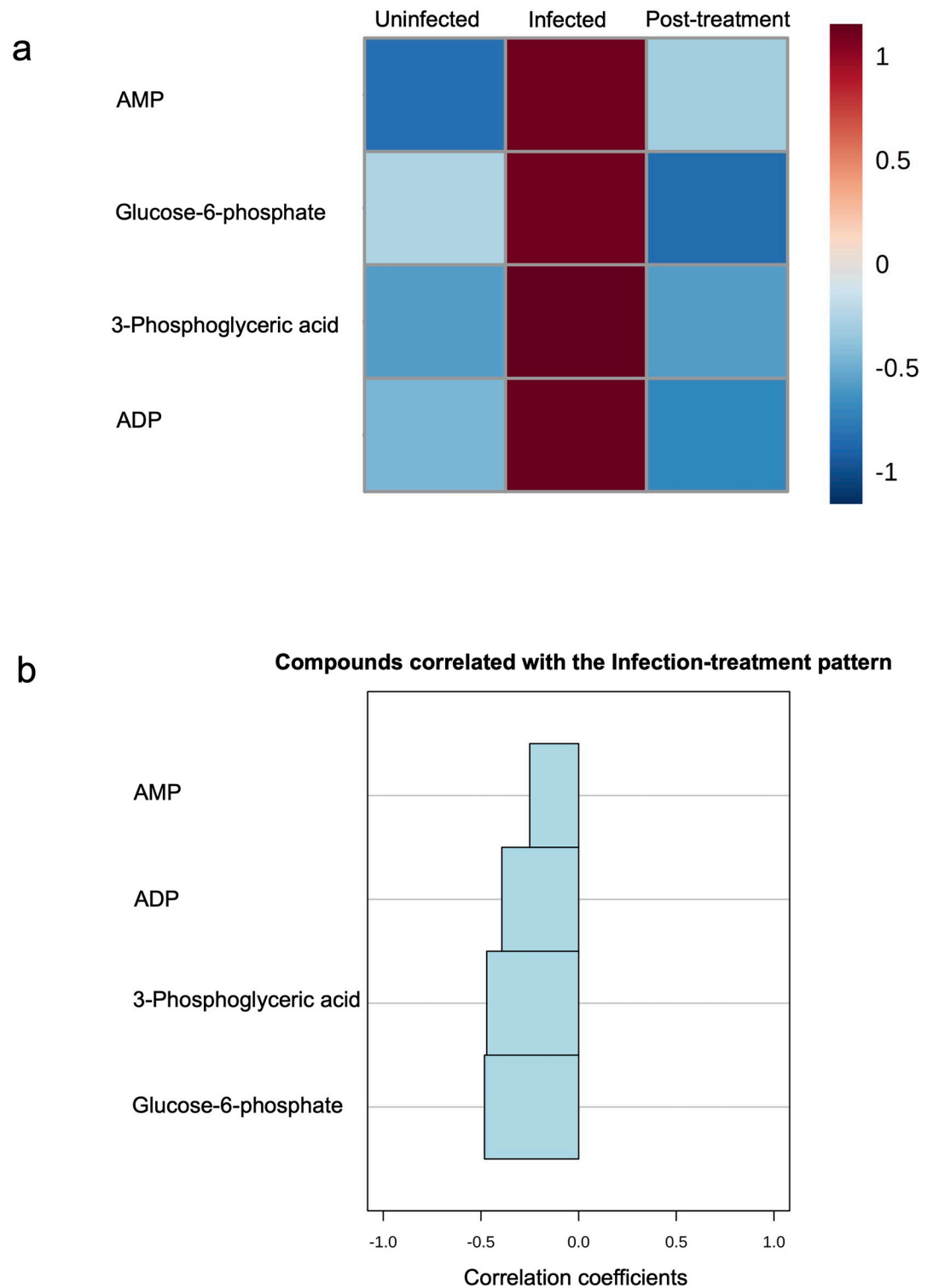
Fig 4. Metabolite concentrations decrease to near-uninfected levels after treatment of infection. a) Heatmap showing the mean concentration patterns of specific metabolites (associated with *S. haematobium* infection status) at pre-infection, infection and at post-treatment. Colour scale (1 to -1) shows Pearson's correlation co-efficient for up-regulated (positive scale) and down-regulated metabolites (negative scale). b) Pattern correlation analysis showing decreasing metabolite concentration patterns from schistosome positive to negative post-treatment (in increasing order of absolute correlation co-efficient). ADP, adenosine diphosphate; AMP, adenosine monophosphate.
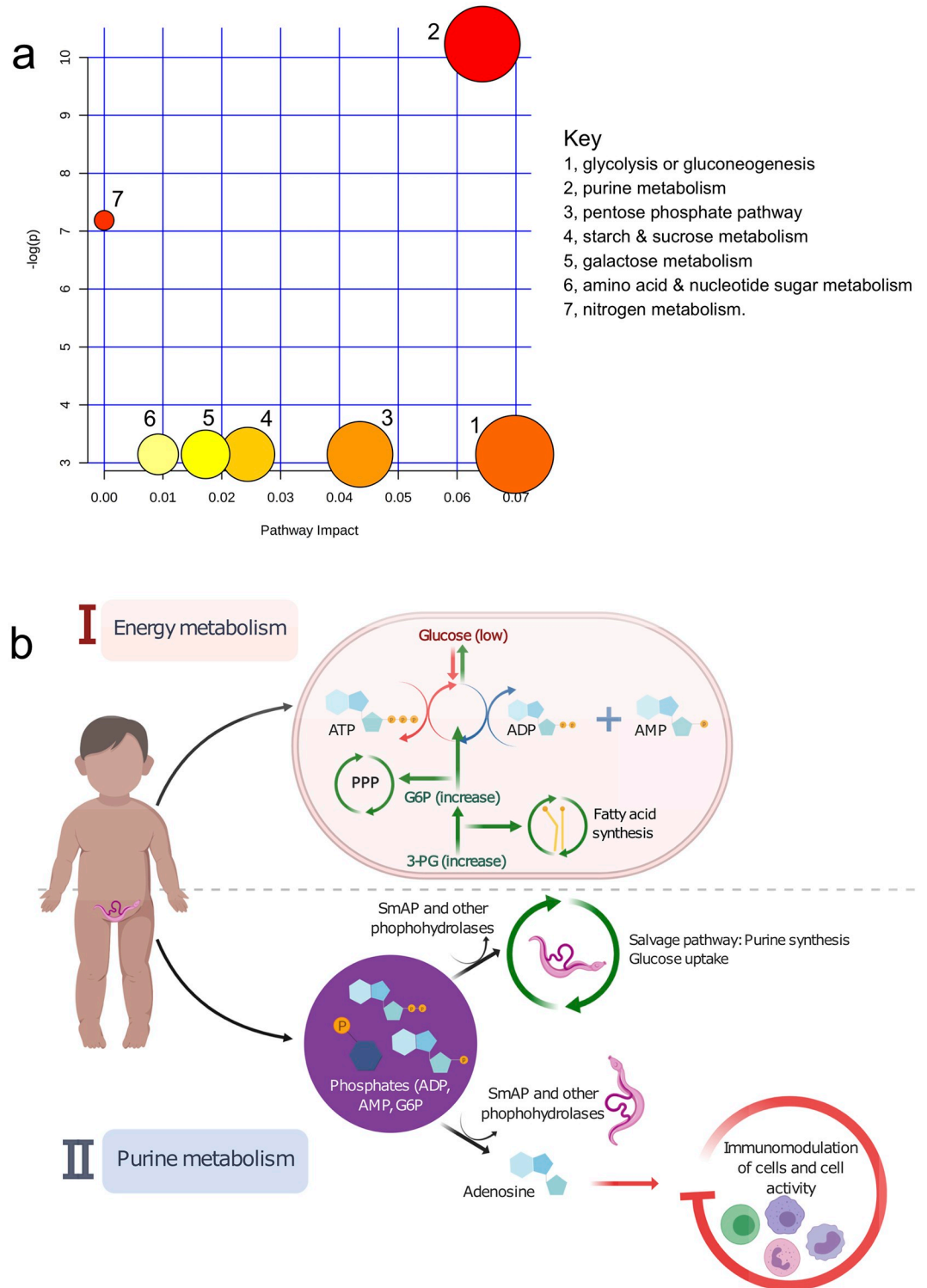
Fig 5. Summary of pathway analysis and biological interpretation for metabolic alterations in early *S. haematobium* infection. a) Pathway map showing the affected metabolic pathways. The map was generated in MetaboAnalyst and shows all matched pathways according to p-values from the pathway enrichment analysis, and pathway impact values from the pathway topology analysis. The size of each circle represents the strength of the impact on the pathway, and significance levels based on p-values range from yellow (least significant) to red (most significant). b) Pathway-based model and interpretation for the affected metabolites and corresponding metabolic pathways during schistosome infection. In response to schistosome

infection and increased demands from the host, there is ↑ glycolysis, ↑ pentose phosphate pathway (PPP), ↑ fatty acid synthesis ↑ gluconeogenesis ↑glycogenolysis, as well as ↑ purine synthesis for salvage by the parasite, leading to the observed increases in the host metabolites identified (i.e. AMP, ADP, 3-PG, and G6P). AMP, adenosine monophosphate; ADP, adenosine diphosphate; ATP, adenosine triphosphate; 3-PG, 3-phosphoglyceric acid; PPP, pentose phosphate pathway; SmAP, schistosome tegumental alkaline phosphatase.

https://doi.org/10.1371/journal.pntd.0008866.g005

or gluconeogenesis, purine metabolism, pentose phosphate pathway (PPP), starch and sucrose metabolism, galactose metabolism, amino acid and nucleotide sugars, and nitrogen metabolism, in order of decreasing impact and statistical significance [details in S11 Table; the statistical p-values from enrichment analysis are further adjusted for multiple pathway testing). Detailed illustrations of the individual metabolism pathways from the analysis are shown in S5 Fig.

Based on the pathway analysis, we proposed a biological interpretation for the metabolite alterations observed (Fig 5B). The adult worm uses large amounts of host glucose and energy [18]. This stimulates host glycolysis and leads to an increase in host ADP and AMP [72,73]. Energy demand for increased protein synthesis could also lead to direct dephosphorylation of adenosine triphosphate (ATP), increasing host AMP. Energy demands from the parasite also increases host glycogenolysis, gluconeogenesis and fatty acid synthesis, increasing the levels of host G6P and 3-PG, essential to enhance the pentose phosphate pathway (PPP) and fatty acid synthesis respectively. In addition schistosome tegumental phosphatases and phosphohydrolases e.g. SmAP [74,75], dephosphorylate the increased exogenous host phosphate molecules (G6P, AMP, ADP), for parasite purine (i.e. adenosine) and glucose uptake. The resulting extra-cellular adenosine is also known to dampen host immunity [76–78] and induce host immuno-modulation [22], both essential for parasite survival.

Discussion

Host-parasite interactions are underpinned by exchange of essential metabolites between the host and the parasite [31–33]. Studies on the host and parasite metabolomes are thus informative on the nature and dynamics of these interactions. While in experimental studies it is possible to infect animals at specific time points, follow the course of infection, and investigate its impact on the host, this is not possible in human hosts. To overcome this challenge, we followed *S. haematobium* infection of populations living in schistosome-endemic areas in Zimbabwe, using a natural infection time-course design. We followed a cohort of Zimbabwean preschool-aged children (≤5 years old) who had never been infected by schistosomes (as confirmed by parasitological diagnosis, guardian interviews and examination of clinical records), to their first schistosome infection and curative treatment. Our study design was informed by knowledge of the exposure patterns to infective water and infection transmission dynamics in the area [79,80] and from previous sero-epidemiology studies in this age group [81,82]. Using a comprehensive mass spectrometry-based approach, we have demonstrated that first infection with the helminth *S. haematobium*, is associated with alterations in host metabolites, primarily linked with energy and purine metabolism. The observed changes were commensurate with increasing infection intensity, a confirmation of an association with the presence of *S. haematobium* infection. Metabolite levels were restored to almost pre-infection levels following curative treatment with the antiheminthic praziquantel.

We analysed the metabolic profiles of children at baseline in order to characterize metabolites in the absence of schistosome infection, as well as to account for confounding factors in subsequent analysis for any metabolite changes upon schistosome infection. Levels of creatinine, citrulline, sarcosine/*N*-methylglycine and GABA were higher in males than females. A potential

explanation for this difference in amino acid metabolites could be differences in weight between the children. In adults, increased amino acid metabolites have been attributed to higher muscle mass in males [83], and this is consistent with the higher weight and associated weight–for-age Z-scores (a standardised assessment of weight in young children, relative to age [84]) in the male children included in this study. There are limited studies on protein and amino acid metabolism in healthy children, and there is a need for further studies to determine if the observations in adults translate to body profiles in young children [85].

We showed that within three months of first schistosome infection in young children, there were significant increases in AMP, ADP, 3-PG, and G6P, compared to uninfected children, and these increases correlated positively with infection intensity. Metabolic pathway analysis showed that the increases were related to energy (glycolysis, PPP, starch, and galactose) and purine metabolism. This is consistent with findings from studies conducted in experimental models of schistosome infection [34,36,86], showing that such host metabolic alterations from schistosome infection begin as early as three weeks post-infection [19].

The observed increases in discriminatory metabolites associated with infection has a physiological explanation. *S. haematobium* predominantly resides in the venous plexus of the bladder with direct access to the flow of nutrients in blood. Experimental studies have shown that the schistosome worm relies on the host's glucose for survival [19]. Every five to six hours, schistosome parasites utilise their dry body weight's worth of glucose from the host, marked by increased lactate and reduced glucose levels in the host blood stream [18,87,88]. Another consequence of schistosome infection is liver injury, as confirmed by histology in experimental studies [19] and in enzymatic human studies [89]. This liver injury is marked by stimulated host glycolysis manifested by reduced plasma glucose as well as glucose and glycogen stores in the liver, as early as 49 days post-infection [34]. Under such nutrient-poor conditions in the host, one of the main results of increased consumption of energy and ATP, is an increase in AMP and ADP, consistent with the findings in the current study [72,73]. AMP and ADP act as sensors for energy homeostasis, helping to activate alternative pathways such as glycogenolysis, gluconeogenesis and fatty acid synthesis to replenish energy stores. Also consistent with our observation of increased AMP is the enhanced energy demand for increased protein synthesis, especially for tRNA activation and guanosine triphosphate regeneration, which results in direct dephosphorylation of even more ATP to AMP by the host system [90]. Parallel to the increased glycolysis, the increased levels of G6P and 3-PG enhances the oxidative phase of the PPP (oxidising even more glucose to produce energy) to generate nicotinamide adenine dinucleotide phosphate (NADPH) for host anabolic reactions, including the biosynthesis of nucleic acids and fatty acids respectively [91]. Although this remains a pathway-based interpretation, our observation of altered energy metabolism pathways including glycolysis and the PPP, are in line with current understanding that such pathways of glucose utilisation are predominantly stimulated during schistosome infection [19,34,36]. Experimental evidence shows that the liver injury caused by schistosome infection [19] is marked by stimulated host glycolysis, manifested by reduced plasma glucose as well as glucose and glycogen stores in the liver [34]. Our results suggest an interplay between the host and the schistosome parasite, consistent with the schistosome-related morbidity observed in young children, including malnutrition, poor growth and poor physical and cognitive performance [14].

Schistosome worms have essential phosphatases and phosphohydrolases such as SmAP, that cleave exogenous phosphates to generate various reaction products [74,75]. In addition, schistosome worms lack *de novo* synthesis of purines and resort to salvaging molecules from the host using these tegumental phosphatases [92], through dephosphorylation and subsequent uptake of reaction products [93]. Thus, the observed increases in AMP, ADP, and G6P are important for parasite purine and energy uptake via phosphate cleavage using tegumental

enzymes. The resulting exogenous molecules such as adenosine has anti-inflammatory properties known to dampen host immunity [76–78]. This would benefit schistosome parasites by creating a less inflammatory and immunologically friendly environment, key to survival of the parasite in the host. Data suggests that such essential functions of parasite phosphatases occur *in vivo* but less *in vitro*, consistent with our hypothesis of the benefits of such molecules for parasite survival in the host [74]. Another direct benefit of the enhanced PPP in generating molecules for fatty acid synthesis in the host is that, schistosomes rely on scavenging lipid precursors from the host to generate phospholipids, due to their inability to synthesise fatty acids *de novo* [94,95]. Schistosome lipids have also been demonstrated to stimulate immunomodulation in the host to enhance parasite survival [96,97].

The correlation between metabolic alterations and increasing egg burden is consistent with experimental studies of metabolic changes being linked to disease progression in schistosome infection [19,35]. In addition, curative treatment with praziquantel in schistosome-positive children showed a decrease in levels of the altered metabolites, three months post-treatment. Consistent with normalisation of affected pathway enzymes upon treatment of schistosome infection in mice models [36], this strengthens the idea that the observed changes are in response to or related to schistosome infection [19]. This observation is also consistent with the fact that curative treatment results in the reversal of early schistosome morbidity/pathology [13,48], and with suggestions that catch-up growth and development is possible in children, following curative praziquantel treatment [98]. We hypothesise that the effect of curative treatment would have been more marked, had the children been surveyed more than three months post-treatment, as it may take longer than that to return to pre-infection levels of the metabolites. The caveat however is that some children could get reinfected if they had been followed up within a longer time frame for post treatment sampling.

Despite allowing for analysis of matching pre- and post-infection samples for the early metabolic responses to the first *S. haematobium* infection in young children, the current study nonetheless had some limitations. Following a natural time-course of first schistosome infections meant that there was no control over the number of infected or uninfected children post-baseline, hence smaller sample sizes especially for schistosome positive individuals. Moreover, the analysis for return of metabolites to pre-infection levels post-treatment might be statistically significant, given a larger sample size for schistosome-positive individuals at three months and at follow up post-treatment. The use of the urine filtration technique for diagnosis, which is dependent on microscopic detection of *S. haematobium* eggs in urine is less sensitive to detecting very low intensity, pre-patent or single sex infections, thus underestimating infection prevalence. However, the current study allows comparison with other studies while parasitological egg count methods remain the predominant schistosome diagnostic in PSAC. Long-term studies relating measurable clinical manifestations of schistosome infection in children to such metabolic alterations, would give a stronger indication of the clinical implications of the schistosome-induced metabolic disturbances.

In conclusion, we show that in a cohort of Zimbabwean preschool-aged children ($\leq$5 years old), the first infection with *S. haematobium* is associated with significant host energy and purine metabolic alterations. These changes correlated with infection intensity and resolved three months post-curative antihelminthic treatment with praziquantel. Our findings are consistent with findings from experimental schistosome studies, as well as observations of parasite-related morbidity, particularly malnutrition, poor growth and poor physical and cognitive performance in schistosome-infected children. Further mechanistic studies will contribute to more understanding of the association between metabolic disturbances and the aetiology of schistosome-related pathology in children, as well as inform the development of appropriate interventions in human helminth infections, such as nutraceuticals in child feeding programs.

Supporting information

S1 Text. Supplementary methods.
(PDF)

S1 Fig. Principal component analysis (PCA) of metabolite features by sex at baseline. a) Scores plot between the selected principal components. The explained variances are shown in brackets. b) Scree plot shows the variance explained by principal components. The green line on top shows the accumulated variance explained; the blue line underneath shows the variance explained by individual principal components.
(TIF)

S2 Fig. OPLSDA model statistics for metabolite features by sex. a) Model overview of the OPLS-DA model for the provided dataset, showing the R^2X, R^2Y and Q^2 coefficients for the groups (Male and Female). b) Permutation analysis, showing the observed and cross-validated R^2Y and Q^2 coefficients.
(TIF)

S3 Fig. Principal component analysis (PCA) of metabolite features by infection status. a) Scores plot between the selected principal components. The explained variances are shown in brackets. b) Scree plot shows the variance explained by principal components. The green line on top shows the accumulated variance explained; the blue line underneath shows the variance explained by individual principal components.
(TIF)

S4 Fig. OPLSDA model statistics for metabolite features by infection status. a) Model overview of the OPLS-DA model for the provided dataset, showing the R^2X, R^2Y and Q^2 coefficients for the groups (schistosome negative and schistosome positive). b) Permutation analysis showing the observed and cross-validated R^2Y and Q^2 coefficients.
(TIF)

S5 Fig. Detailed metabolic pathways of discriminatory metabolites for schistosome infection. a) Glycolysis/Gluconeogenesis (hits = glucose-6-phosphate). b) Purine metabolism (hits = AMP, ADP). c) Pentose phosphate pathway (hits = glucose-6-phosphate). d) Starch and sucrose metabolism (hits = glucose-6-phosphate). e) Galactose metabolism (hits = glucose-6-phosphate). f) Nitrogen metabolism (hits = glucose-6-phosphate). g) Amino, sugar and nucleotide metabolism (hits = glucose-6-phosphate). For compound colours within each metabolic pathway map–light blue are metabolites not in the data set used for pathway analysis and are used as background for enrichment analysis; other colours (varying from yellow to red) means the metabolites are in the data with different levels of significance. AMP, adenosine monophosphate; ADP, adenosine diphosphate.
(TIF)

S1 Table. Baseline MANOVA output for influence of age and sex on metabolite profiles.
(PDF)

S2 Table. Important metabolites identified from fold change analysis by sex.
(PDF)

S3 Table. Correlation pattern analysis of metabolites showing a female to male pattern.
(PDF)

S4 Table. Output from OPLSDA model S-plot for sex, along with corresponding VIP values.
(PDF)

S5 Table. Follow-up MANOVA output for influence of infection on metabolite profiles.
(PDF)

S6 Table. Important metabolites identified from fold change analysis by infection status.
(PDF)

S7 Table. Correlation pattern analysis of compounds showing patterns from negative to positive for infection.
(PDF)

S8 Table. Output from OPLSDA model S-plot for infection, along with corresponding VIP values.
(PDF)

S9 Table. MANOVA output for influence of infection intensity on metabolite profiles.
(PDF)

S10 Table. Correlation pattern analysis of metabolites showing patterns from positive for infection to negative post-treatment.
(PDF)

S11 Table. Analysis output from metabolite pathway analysis.
(PDF)

Acknowledgments

Author Contributions

Conceptualization: Derick N. M. Osakunor, Takafira Mduluza, Mark E. J. Woolhouse, Francisca Mutapi.

Data curation: Derick N. M. Osakunor.

Formal analysis: Derick N. M. Osakunor, Douglas Osei-Hyiaman, Karl Burgess, Francisca Mutapi.

Investigation: Derick N. M. Osakunor, Takafira Mduluza, Douglas Osei-Hyiaman, Karl Burgess, Francisca Mutapi.

Methodology: Derick N. M. Osakunor, Takafira Mduluza, Mark E. J. Woolhouse, Francisca Mutapi.

Project administration: Takafira Mduluza, Francisca Mutapi.

Validation: Derick N. M. Osakunor, Douglas Osei-Hyiaman, Karl Burgess, Mark E. J. Woolhouse, Francisca Mutapi.

Visualization: Derick N. M. Osakunor.

Writing – original draft: Derick N. M. Osakunor.

Writing – review & editing: Derick N. M. Osakunor, Takafira Mduluza, Douglas Osei-Hyia-man, Karl Burgess, Mark E. J. Woolhouse, Francisca Mutapi.

References

1. Hotez PJ, Alvarado M, Basanez MG, Bolliger I, Bourne R, Boussinesq M, et al. The global burden of disease study 2010: interpretation and implications for the neglected tropical diseases. PLoS Negl Trop Dis. 2014; 8(7):e2865. Epub 2014/07/25. https://doi.org/10.1371/journal.pntd.0002865 PMID: 25058013

2. de Silva NR, Brooker S, Hotez PJ, Montresor A, Engels D, Savioli L. Soil-transmitted helminth infections: updating the global picture. Trends Parasitol. 2003; 19(12):547–51. https://doi.org/10.1016/j.pt.2003.10.002 PMID: 14642761

3. Hotez P, Raff S, Fenwick A, Richards F Jr., Molyneux DH. Recent progress in integrated neglected tropical disease control. Trends Parasitol. 2007; 23(11):511–4. https://doi.org/10.1016/j.pt.2007.08.015 PMID: 17951109

4. WHO Expert Committee. Prevention and control of schistosomiasis and soil-transmitted helminthiasis. World Health Organ Tech Rep Ser. 2002; 912:i–vi, 1–57, back cover. PMID: 12592987

5. World Health Organization. Female genital schistosomiasis: A pocket atlas for clinical health-care professionals. 2015.

6. Steinmann P, Keiser J, Bos R, Tanner M, Utzinger J. Schistosomiasis and water resources development: systematic review, meta-analysis, and estimates of people at risk. Lancet Infect Dis. 2006; 6 (7):411–25. https://doi.org/10.1016/S1473-3099(06)70521-7 PMID: 16790382

7. World Health Organization. Schistosomiasis: World Health Organization (WHO); 2020 [updated 2/03/2020; cited 2020 09/03]. https://www.who.int/news-room/fact-sheets/detail/schistosomiasis.

8. van der Werf MJ, de Vlas SJ, Brooker S, Looman CW, Nagelkerke NJ, Habbema JD, et al. Quantification of clinical morbidity associated with schistosome infection in sub-Saharan Africa. Acta Trop. 2003; 86(2–3):125–39. https://doi.org/10.1016/s0001-706x(03)00029-9 PMID: 12745133

9. McManus DP, Dunne DW, Sacko M, Utzinger J, Vennervald BJ, Zhou XN. Schistosomiasis. Nat Rev Dis Primers. 2018; 4(1):13. https://doi.org/10.1038/s41572-018-0013-8 PMID: 30093684

10. Woolhouse ME, Mutapi F, Ndhlovu PD, Chandiwana SK, Hagan P. Exposure, infection and immune responses to *Schistosoma haematobium* in young children. Parasitology. 2000; 120 (Pt 1):37–44. https://doi.org/10.1017/s0031182099005156 PMID: 10726264

11. Wilkins HA, Goll P, Marshall TF, Moore P. The significance of proteinuria and haematuria in *Schistosoma haematobium* infection. Trans R Soc Trop Med Hyg. 1979; 73(1):74–80. https://doi.org/10.1016/0035-9203(79)90134-2 PMID: 442186

12. Wami WM, Nausch N, Midzi N, Gwisai R, Mduluza T, Woolhouse M, et al. Identifying and evaluating field indicators of urogenital schistosomiasis-related morbidity in preschool-aged children. PLoS Negl Trop Dis. 2015; 9(3):e0003649. https://doi.org/10.1371/journal.pntd.0003649 PMID: 25793584

13. Osakunor DNM, Mduluza T, Midzi N, Chase-Topping M, Mutsaka-Makuvaza MJ, Chimponda T, et al. Dynamics of paediatric urogenital schistosome infection, morbidity and treatment: a longitudinal study among preschool children in Zimbabwe. BMJ Glob Health. 2018; 3(2):e000661. https://doi.org/10.1136/bmjgh-2017-000661 PMID: 29616147

14. Freer JB, Bourke CD, Durhuus GH, Kjetland EF, Prendergast AJ. Schistosomiasis in the first 1000 days. Lancet Infect Dis. 2018; 18(6):e193–e203. https://doi.org/10.1016/S1473-3099(17)30490-5 PMID: 29170089

15. Tuffour I, Ayi I, Gwira TM, Dumashie E, Ashong Y, Appiah-Opong R. Schistosoma Egg Antigen Induces Oncogenic Alterations in Human Prostate Cells. Anal Cell Pathol (Amst). 2018; 2018:4675380. Epub 2019/01/12. https://doi.org/10.1155/2018/4675380 PMID: 30631746

16. Gelfand M, Weinberg R, Castle W. Relation between carcinoma of the bladder and infestation with *Schistosoma haematobium*. The Lancet. 1967; 289(7502):1249–51. https://doi.org/10.1016/s0140-6736(67)92714-6 PMID: 4165038

17. Lichtenberg FV. Schistosomiasis as a Worldwide Problem—Pathology. J Toxicol Env Health. 1975; 1 (2):175–84.

18. Bueding E. Carbohydrate metabolism of *Schistosoma mansoni*. J Gen Physiol. 1950; 33(5):475–95. https://doi.org/10.1085/jgp.33.5.475 PMID: 15422103

19. Wu J, Xu W, Ming Z, Dong H, Tang H, Wang Y. Metabolic changes reveal the development of schistosomiasis in mice. PLoS Negl Trop Dis. 2010; 4(8). https://doi.org/10.1371/journal.pntd.0000807 PMID: 20824219

20.   Pearce EJ, MacDonald AS. The immunobiology of schistosomiasis. Nat Rev Immunol. 2002; 2(7):499–511. https://doi.org/10.1038/nri843 PMID: 12094224

21.   Colley DG, Secor WE. Immunology of human schistosomiasis. Parasite Immunol. 2014; 36(8):347–57. https://doi.org/10.1111/pim.12087 PMID: 25142505

22.   van Riet E, Hartgers FC, Yazdanbakhsh M. Chronic helminth infections induce immunomodulation: consequences and mechanisms. Immunobiology. 2007; 212(6):475–90. https://doi.org/10.1016/j.imbio.2007.03.009 PMID: 17544832

23.   van der Zande HJP, Zawistowska-Deniziak A, Guigas B. Immune Regulation of Metabolic Homeostasis by Helminths and Their Molecules. Trends Parasitol. 2019; 35(10):795–808. Epub 2019/09/08. https://doi.org/10.1016/j.pt.2019.07.014 PMID: 31492623

24.   Brestoff JR, Artis D. Immune regulation of metabolic homeostasis in health and disease. Cell. 2015; 161(1):146–60. Epub 2015/03/31. https://doi.org/10.1016/j.cell.2015.02.022 PMID: 25815992

25.   Saule P, Adriaenssens E, Delacre M, Chassande O, Bossu M, Auriault C, et al. Early variations of host thyroxine and interleukin-7 favor Schistosoma mansoni development. J Parasitol. 2002; 88(5):849–55.

26.   de Mendonca RL, Escriva H, Bouton D, Laudet V, Pierce RJ. Hormones and nuclear receptors in schistosome development. Parasitol Today. 2000; 16(6):233–40. https://doi.org/10.1016/s0169-4758(00)01641-0 PMID: 10827428

27.   You H, Gobert GN, Cai P, Mou R, Nawaratna S, Fang G, et al. Suppression of the Insulin Receptors in Adult Schistosoma japonicum Impacts on Parasite Growth and Development: Further Evidence of Vaccine Potential. PLoS Negl Trop Dis. 2015; 9(5):e0003730. https://doi.org/10.1371/journal.pntd.0003730 PMID: 25961574

28.   Amiri P, Locksley RM, Parslow TG, Sadick M, Rector E, Ritter D, et al. Tumour necrosis factor alpha restores granulomas and induces parasite egg-laying in schistosome-infected SCID mice. Nature. 1992; 356(6370):604–7. https://doi.org/10.1038/356604a0 PMID: 1560843

29.   Davies SJ, Lim KC, Blank RB, Kim JH, Lucas KD, Hernandez DC, et al. Involvement of TNF in limiting liver pathology and promoting parasite survival during schistosome infection. Int J Parasitol. 2004; 34(1):27–36. https://doi.org/10.1016/j.ijpara.2003.10.010 PMID: 14711587

30.   Davies SJ, Grogan JL, Blank RB, Lim KC, Locksley RM, McKerrow JH. Modulation of blood fluke development in the liver by hepatic CD4+ lymphocytes. Science. 2001; 294(5545):1358–61. Epub 2001/11/10. https://doi.org/10.1126/science.1064462 PMID: 11701932

31.   Tang H, Ming Z, Liu R, Xiong T, Grevelding CG, Dong H, et al. Development of adult worms and granulomatous pathology are collectively regulated by T- and B-cells in mice infected with Schistosoma japonicum. PLoS One. 2013; 8(1):e54432. https://doi.org/10.1371/journal.pone.0054432 PMID: 23349889

32.   Cheng YL, Song WJ, Liu WQ, Lei JH, Mo HM, Ruppel A, et al. The effects of T cell deficiency on the development of worms and granuloma formation in mice infected with Schistosoma japonicum. Parasitol Res. 2008; 102(6):1129–34. https://doi.org/10.1007/s00436-008-0880-0 PMID: 18246371

33.   Lamb EW, Walls CD, Pesce JT, Riner DK, Maynard SK, Crow ET, et al. Blood fluke exploitation of noncognate CD4+ T cell help to facilitate parasite development. PLoS Pathog. 2010; 6(4):e1000892. https://doi.org/10.1371/journal.ppat.1000892 PMID: 20442785

34.   Wang Y, Holmes E, Nicholson JK, Cloarec O, Chollet J, Tanner M, et al. Metabonomic investigations in mice infected with Schistosoma mansoni: an approach for biomarker identification. Proc Natl Acad Sci U S A. 2004; 101(34):12676–81. https://doi.org/10.1073/pnas.0404878101 PMID: 15314235

35.   Li JV, Holmes E, Saric J, Keiser J, Dirnhofer S, Utzinger J, et al. Metabolic profiling of a Schistosoma mansoni infection in mouse tissues using magic angle spinning-nuclear magnetic resonance spectroscopy. Int J Parasitol. 2009; 39(5):547–58. https://doi.org/10.1016/j.ijpara.2008.10.010 PMID: 19068218

36.   Ahmed SA, Gad MZ. Effect of schistosomal infection and its treatment on some key enzymes of glucose metabolism in mice livers. Arzneimittelforschung. 1995; 45(12):1324–8. PMID: 8595093

37.   Garcia-Perez I, Whitfield P, Bartlett A, Angulo S, Legido-Quigley C, Hanna-Brown M, et al. Metabolic fingerprinting of Schistosoma mansoni infection in mice urine with capillary electrophoresis. Electrophoresis. 2008; 29(15):3201–6. https://doi.org/10.1002/elps.200800031 PMID: 18633941

38.   Panic G, Coulibaly JT, Harvey N, Keiser J, Swann J. Characterizing the Biochemical Response to Schistosoma mansoni Infection and Treatment with Praziquantel in Preschool and School Aged Children. J Proteome Res. 2018; 17(6):2028–33. https://doi.org/10.1021/acs.jproteome.7b00910 PMID: 29701975

39.   Balog CI, Meissner A, Goraler S, Bladergroen MR, Vennervald BJ, Mayboroda OA, et al. Metabonomic investigation of human Schistosoma mansoni infection. Mol Biosyst. 2011; 7(5):1473–80. https://doi.org/10.1039/c0mb00262c PMID: 21336380

40. Stanley RG, Jackson CL, Griffiths K, Doenhoff MJ. Effects of *Schistosoma mansoni* worms and eggs on circulating cholesterol and liver lipids in mice. Atherosclerosis. 2009; 207(1):131–8. https://doi.org/10.1016/j.atherosclerosis.2009.04.037 PMID: 19464685

41. Zaccone P, Fehervari Z, Jones FM, Sidobre S, Kronenberg M, Dunne DW, et al. S*chistosoma mansoni* antigens modulate the activity of the innate immune response and prevent onset of type 1 diabetes. Eur J Immunol. 2003; 33(5):1439–49. https://doi.org/10.1002/eji.200323910 PMID: 12731071

42. Chen Y, Lu J, Huang Y, Wang T, Xu Y, Xu M, et al. Association of previous schistosome infection with diabetes and metabolic syndrome: a cross-sectional study in rural China. J Clin Endocrinol Metab. 2013; 98(2):E283–7. https://doi.org/10.1210/jc.2012-2517 PMID: 23275524

43. Wolde M, Berhe N, Medhin G, Chala F, van Die I, Tsegaye A. Inverse Associations of *Schistosoma mansoni* Infection and Metabolic Syndromes in Humans: A Cross-Sectional Study in Northeast Ethiopia. Microbiol Insights. 2019; 12:1178636119849934. https://doi.org/10.1177/1178636119849934 PMID: 31205419

44. Rollinson D. A wake up call for urinary schistosomiasis: reconciling research effort with public health importance. Parasitology. 2009; 136(12):1593–610. https://doi.org/10.1017/S0031182009990552 PMID: 19627633

45. Midzi N, Mduluza T, Chimbari MJ, Tshuma C, Charimari L, Mhlanga G, et al. Distribution of schistosomiasis and soil transmitted helminthiasis in Zimbabwe: towards a national plan of action for control and elimination. PLoS Negl Trop Dis. 2014; 8(8):e3014. https://doi.org/10.1371/journal.pntd.0003014 PMID: 25121489

46. Webbe G, James C. A comparison of two geographical strains of *Schistosoma haematobium*. J Helminthol. 1971; 45(2):271–84. PMID: 5123704

47. Smith M, Clegg JA, Webbe G. Culture of *Schistosoma haematobium* in vivo and in vitro. Ann Trop Med Parasitol. 1976; 70(1):101–7. https://doi.org/10.1080/00034983.1976.11687100 PMID: 1267504

48. Wami WM, Nausch N, Midzi N, Gwisai R, Mduluza T, Woolhouse MEJ, et al. Comparative Assessment of Health Benefits of Praziquantel Treatment of Urogenital Schistosomiasis in Preschool and Primary School-Aged Children. Biomed Res Int. 2016. Artn 9162631 https://doi.org/10.1155/2016/9162631 PMID: 27631011

49. Mott KE, Baltes R, Bambagha J, Baldassini B. Field studies of a reusable polyamide filter for detection of *Schistosoma haematobium* eggs by urine filtration. Tropenmed Parasitol. 1982; 33(4):227–8. PMID: 7164164

50. Katz N, Chaves A, Pellegrino J. A simple device for quantitative stool thick-smear technique in *Schistosomiasis mansoni*. Rev Inst Med Trop Sao Paulo. 1972; 14(6):397–400. PMID: 4675644

51. Yin PY, Lehmann R, Xu GW. Effects of pre-analytical processes on blood samples used in metabolomics studies. Anal Bioanal Chem. 2015; 407(17):4879–92. https://doi.org/10.1007/s00216-015-8565-x PMID: 25736245

52. Kim K, Mall C, Taylor SL, Hitchcock S, Zhang C, Wettersten HI, et al. Mealtime, temporal, and daily variability of the human urinary and plasma metabolomes in a tightly controlled environment. PLoS One. 2014; 9(1):e86223. https://doi.org/10.1371/journal.pone.0086223 PMID: 24475090

53. Mitsuishi Y, Taguchi K, Kawatani Y, Shibata T, Nukiwa T, Aburatani H, et al. Nrf2 Redirects Glucose and Glutamine into Anabolic Pathways in Metabolic Reprogramming. Cancer Cell. 2012; 22(1):66–79. https://doi.org/10.1016/j.ccr.2012.05.016 PMID: 22789539

54. Ohashi Y, Hirayama A, Ishikawa T, Nakamura S, Shimizu K, Ueno Y, et al. Depiction of metabolome changes in histidine-starved Escherichia coli by CE-TOFMS. Mol Biosyst. 2008; 4(2):135–47. https://doi.org/10.1039/b714176a PMID: 18213407

55. Soga T, Heiger DN. Amino acid analysis by capillary electrophoresis electrospray ionization mass spectrometry. Anal Chem. 2000; 72(6):1236–41. https://doi.org/10.1021/ac990976y PMID: 10740865

56. Soga T, Ohashi Y, Ueno Y, Naraoka H, Tomita M, Nishioka T. Quantitative metabolome analysis using capillary electrophoresis mass spectrometry. Journal of Proteome Research. 2003; 2(5):488–94. https://doi.org/10.1021/pr034020m PMID: 14582645

57. Soga T, Ueno Y, Naraoka H, Ohashi Y, Tomita M, Nishioka T. Simultaneous determination of anionic intermediates for Bacillus subtilis metabolic pathways by capillary electrophoresis electrospray ionization mass spectrometry. Anal Chem. 2002; 74(10):2233–9. https://doi.org/10.1021/ac020064n PMID: 12038746

58. Chong J, Soufan O, Li C, Caraus I, Li S, Bourque G, et al. MetaboAnalyst 4.0: towards more transparent and integrative metabolomics analysis. Nucleic Acids Res. 2018; 46(W1):W486–W94. https://doi.org/10.1093/nar/gky310 PMID: 29762782

59. Xia J, Psychogios N, Young N, Wishart DS. MetaboAnalyst: a web server for metabolomic data analysis and interpretation. Nucleic Acids Res. 2009; 37(Web Server issue):W652–60. https://doi.org/10.1093/nar/gkp356 PMID: 19429898

60. Xia J, Wishart DS. Web-based inference of biological patterns, functions and pathways from metabolomic data using MetaboAnalyst. Nature Protocols. 2011; 6:743. https://doi.org/10.1038/nprot.2011.319 PMID: 21637195

61. van den Berg RA, Hoefsloot HC, Westerhuis JA, Smilde AK, van der Werf MJ. Centering, scaling, and transformations: improving the biological information content of metabolomics data. BMC Genomics. 2006; 7:142. https://doi.org/10.1186/1471-2164-7-142 PMID: 16762068

62. Mutapi F, Roddam A. p values for pathogens: statistical inference from infectious-disease data. Lancet Infect Dis. 2002; 2(4):219–30. https://doi.org/10.1016/s1473-3099(02)00240-2 PMID: 11937422

63. Benjamini Y, Hochberg Y. Controlling the false discovery rate: a practical and powerful approach to multiple testing. Journal of the Royal statistical society: Series B (Methodological). 1995; 57(1):289–300.

64. Patterson TA, Lobenhofer EK, Fulmer-Smentek SB, Collins PJ, Chu TM, Bao W, et al. Performance comparison of one-color and two-color platforms within the MicroArray Quality Control (MAQC) project. Nat Biotechnol. 2006; 24(9):1140–50. https://doi.org/10.1038/nbt1242 PMID: 16964228

65. Wiklund S, Johansson E, Sjostrom L, Mellerowicz EJ, Edlund U, Shockcor JP, et al. Visualization of GC/TOF-MS-based metabolomics data for identification of biochemically interesting compounds using OPLS class models. Analytical Chemistry. 2008; 80(1):115–22. https://doi.org/10.1021/ac0713510 PMID: 18027910

66. Wold S, Antti H, Lindgren F, Ohman J. Orthogonal signal correction of near-infrared spectra. Chemometr Intell Lab. 1998; 44(1–2):175–85. https://doi.org/10.1016/S0169-7439(98)00109-9

67. Singer BH, Utzinger J, Ryff CD, Wang Y, Holmes E, Nicholson J. Exploiting the potential of metabonomics in large population studies: three venues. The handbook of metabonomics and metabolomics: Elsevier BV; 2007. p. 289–325.

68. Wold S, Sjostrom M, Eriksson L. PLS-regression: a basic tool of chemometrics. Chemometr Intell Lab. 2001; 58(2):109–30. https://doi.org/10.1016/S0169-7439(01)00155-1

69. Szymanska E, Saccenti E, Smilde AK, Westerhuis JA. Double-check: validation of diagnostic statistics for PLS-DA models in metabolomics studies. Metabolomics. 2012; 8(Suppl 1):3–16. https://doi.org/10.1007/s11306-011-0330-3 PMID: 22593721

70. Wheelock AM, Wheelock CE. Trials and tribulations of 'omics data analysis: assessing quality of SIMCA-based multivariate models using examples from pulmonary medicine. Mol Biosyst. 2013; 9 (11):2589–96. https://doi.org/10.1039/c3mb70194h PMID: 23999822

71. Mondal D, Minak J, Alam M, Liu Y, Dai J, Korpe P, et al. Contribution of enteric infection, altered intestinal barrier function, and maternal malnutrition to infant malnutrition in Bangladesh. Clin Infect Dis. 2012; 54(2):185–92. https://doi.org/10.1093/cid/cir807 PMID: 22109945

72. Carling D, Thornton C, Woods A, Sanders MJ. AMP-activated protein kinase: new regulation, new roles? Biochem J. 2012; 445(1):11–27. Epub 2012/06/19. https://doi.org/10.1042/BJ20120546 PMID: 22702974

73. Hardie DG, Ross FA, Hawley SA. AMPK: a nutrient and energy sensor that maintains energy homeostasis. Nat Rev Mol Cell Biol. 2012; 13(4):251–62. Epub 2012/03/23. https://doi.org/10.1038/nrm3311 PMID: 22436748

74. Bhardwaj R, Skelly PJ. Characterization of schistosome tegumental alkaline phosphatase (SmAP). PLoS Negl Trop Dis. 2011; 5(4):e1011. https://doi.org/10.1371/journal.pntd.0001011 PMID: 21483710

75. Cesari IM, Simpson AJ, Evans WH. Properties of a series of tegumental membrane-bound phosphohydrolase activities of *Schistosoma mansoni*. Biochem J. 1981; 198(3):467–73. https://doi.org/10.1042/bj1980467 PMID: 6275849

76. Bours MJ, Swennen EL, Di Virgilio F, Cronstein BN, Dagnelie PC. Adenosine 5'-triphosphate and adenosine as endogenous signaling molecules in immunity and inflammation. Pharmacol Ther. 2006; 112 (2):358–404. https://doi.org/10.1016/j.pharmthera.2005.04.013 PMID: 16784779

77. Gessi S, Varani K, Merighi S, Fogli E, Sacchetto V, Benini A, et al. Adenosine and lymphocyte regulation. Purinergic Signal. 2007; 3(1–2):109–16. https://doi.org/10.1007/s11302-006-9042-y PMID: 18404424

78. Hasko G, Cronstein BN. Adenosine: an endogenous regulator of innate immunity. Trends Immunol. 2004; 25(1):33–9. https://doi.org/10.1016/j.it.2003.11.003 PMID: 14698282

79. Mutsaka-Makuvaza MJ, Matsena-Zingoni Z, Katsidzira A, Tshuma C, Chin'ombe N, Zhou XN, et al. Urogenital schistosomiasis and risk factors of infection in mothers and preschool children in an endemic district in Zimbabwe. Parasit Vectors. 2019; 12(1):427. Epub 2019/09/04. https://doi.org/10.1186/s13071-019-3667-5 PMID: 31477172

80. Mutsaka-Makuvaza MJ, Matsena-Zingoni Z, Tshuma C, Ray S, Zhou XN, Webster B, et al. Reinfection of urogenital schistosomiasis in pre-school children in a highly endemic district in Northern Zimbabwe: a

12 months compliance study. Infect Dis Poverty. 2018; 7(1):102. Epub 2018/10/01. https://doi.org/10.1186/s40249-018-0483-7 PMID: 30268157

81. Rujeni N, Nausch N, Midzi N, Cowan GJ, Burchmore R, Cavanagh DR, et al. Immunological consequences of antihelminthic treatment in preschool children exposed to urogenital schistosome infection. J Trop Med. 2013; 2013:283619. https://doi.org/10.1155/2013/283619 PMID: 23840222

82. Wami WM, Nausch N, Bauer K, Midzi N, Gwisai R, Simmonds P, et al. Comparing parasitological vs serological determination of *Schistosoma haematobium* infection prevalence in preschool and primary school-aged children: implications for control programmes. Parasitology. 2014; 141(14):1962–70. https://doi.org/10.1017/S0031182014000213 PMID: 24679476

83. Lukaski HC. Estimation of muscle mass. In: Roche AF HS, Lohman TG, editor. Human Body Composition. Champaign, IL: HumanKinetics; 1996. p. 109–28.

84. MOH Malawi. Guidelines for Community-Based Management of Acute Malnutrition. Lilongwe, Malawi: Ministry of Health, 2016.

85. Markofski MM, Volpi E. Protein metabolism in women and men: similarities and disparities. Curr Opin Clin Nutr Metab Care. 2011; 14(1):93–7. Epub 2010/11/20. https://doi.org/10.1097/MCO.0b013e3283412343 PMID: 21088570

86. Liu R, Cheng WJ, Tang HB, Zhong QP, Ming ZP, Dong HF. Comparative Metabonomic Investigations of *Schistosoma japonicum* From SCID Mice and BALB/c Mice: Clues to Developmental Abnormality of Schistosome in the Immunodeficient Host. Front Microbiol. 2019; 10:440. https://doi.org/10.3389/fmicb.2019.00440 PMID: 30915055

87. Bueding E, Fisher J. Metabolic requirements of schistosomes. J Parasitol. 1982; 68(2):208–12. PMID: 7077454

88. Schiller EL, Bueding E, Turner VM, Fisher J. Aerobic and anaerobic carbohydrate metabolism and egg production of *Schistosoma mansoni* in vitro. J Parasitol. 1975; 61(3):385–89. PMID: 1169294

89. Abdel-Rahim IM, Kaiser C, Homeida M, Elsheikh M, Schmidt E, Ehrich JH, et al. Enzyme activities and protein concentrations in serum of patients with hepatosplenic schistosomiasis. Trop Med Parasitol. 1990; 41(3):262–4. Epub 1990/09/01. PMID: 1701559

90. Pontes MH, Sevostyanova A, Groisman EA. When too much ATP is bad for protein synthesis. Journal of molecular biology. 2015; 427(16):2586–94. https://doi.org/10.1016/j.jmb.2015.06.021 PMID: 26150063

91. Eggleston LV, Krebs HA. Regulation of the pentose phosphate cycle. Biochem J. 1974; 138(3):425–35. Epub 1974/03/01. https://doi.org/10.1042/bj1380425 PMID: 4154743

92. Levy MG, Read CP. Purine and pyrimidine transport in *Schistosoma mansoni*. J Parasitol. 1975; 61 (4):627–32. PMID: 1165547

93. Levy MG, Read CP. Relation of tegumentary phosphohydrolase to purine and pyrimidine transport in *Schistosoma mansoni*. J Parasitol. 1975; 61(4):648–56. PMID: 170394

94. Meyer F, Meyer H, Bueding E. Lipid metabolism in the parasitic and free-living flatworms, *Schistosoma mansoni* and Dugesia dorotocephala. Biochim Biophys Acta. 1970; 210(2):257–66. https://doi.org/10.1016/0005-2760(70)90170-0 PMID: 4319989

95. Brouwers JF, Smeenk IM, van Golde LM, Tielens AG. The incorporation, modification and turnover of fatty acids in adult *Schistosoma mansoni*. Mol Biochem Parasitol. 1997; 88(1–2):175–85. https://doi.org/10.1016/s0166-6851(97)00091-1 PMID: 9274878

96. Giera M, Kaisar MMM, Derks RJE, Steenvoorden E, Kruize YCM, Hokke CH, et al. The *Schistosoma mansoni* lipidome: Leads for immunomodulation. Anal Chim Acta. 2018; 1037:107–18. https://doi.org/10.1016/j.aca.2017.11.058 PMID: 30292284

97. van der Kleij D, Latz E, Brouwers JF, Kruize YC, Schmitz M, Kurt-Jones EA, et al. A novel host-parasite lipid cross-talk. Schistosomal lyso-phosphatidylserine activates toll-like receptor 2 and affects immune polarization. J Biol Chem. 2002; 277(50):48122–9. https://doi.org/10.1074/jbc.M206941200 PMID: 12359728

98. Gurarie D, Wang X, Bustinduy AL, King CH. Modeling the effect of chronic schistosomiasis on childhood development and the potential for catch-up growth with different drug treatment strategies promoted for control of endemic schistosomiasis. Am J Trop Med Hyg. 2011; 84(5):773–81. https://doi.org/10.4269/ajtmh.2011.10-0642 PMID: 21540388